Journal of Thermal Analysis and Calorimetry, Vol. 71 (2003) 715–726

STUDY OF NATURAL AND ION EXCHANGED VERMICULITE BY EMANATION THERMAL ANALYSIS, TG, DTA AND XRD

L. A. Pérez-Maqueda[1], V. Balek[2], J. Poyato[1], J. L. Pérez-Rodríquez[1], J. Šubrt[3], I. M. Bountsewa[4], I. N. Beckman[4] and Z. Málek[2]*

[1]Instituto de Ciencia de Materiales de Sevilla. CSIC-UNSE. c/. Américo Vespucio, s/n. 41092 Sevilla, Spain
[2]Nuclear Research Institute Rez, CZ-25068 Řež, Czech Republic
[3]Institute of Inorganic Chemistry AS CR, CZ-250 68 Řež, Czech Republic
[4]Faculty of Chemistry, Moscow State University, Moscow 199234, Russia

Abstract

Emanation thermal analysis (ETA), thermogravimetry, DTA and XRD were used in thermal characterization of natural vermiculite (Santa Olalla, Huelva, Spain) and of Na^+- and NH_4^+- exchanged vermiculite samples during heating in air in the range 25–1100°C. A good agreement between the results of these methods was found. Changes in the radon release rate measured by ETA, which reflected the decrease and collapse of the interlayer space after the release of water as well as the formation of new crystalline phases were evaluated using a mathematical model. The model used for the evaluation was found suitable for the quantitative characterization of microstructure changes during in situ conditions of heating of vermiculite samples.

Keywords: emanation thermal analysis, DTA, ion exchange, microstructure, TG, vermiculite, XRD

Introduction

Thermal behaviour of vermiculite was investigated by numerous authors, e.g. [1–4]. It is well known that vermiculites consist of unit layers composed from two silica tetrahedral sheets attached to a central magnesium octahedral sheet. Al^{3+} for Si^{4+} substitution in tetrahedral layers, and Al^{3+} and/or Fe^{3+} for Mg^{2+} substitutions in octahedral layers are responsible for the negative charge of the structure.

The ETA [5–7] was already applied in the characterization of microstructure changes of other smectite clays, such as beidellite, saponite, hectorite [8] and montmorillonite, saturated with various cations [9], as well as hydroxyaluminium pillared montmorillonite [10]. It brought about supplementary information to that obtained by DTA and TG characterizing the effect of Na^+ and NH_4^+ cations on thermal behaviour of natural Mg vermiculite [11].

* Author for correspondence: E-mail: bal@ujv.cz

1388–6150/2003/ $ 20.00

Akadémiai Kiadó, Budapest
Kluwer Academic Publishers, Dordrecht

In this study we used the mathematical model [12] in order to evaluate the microstructure changes of natural and ion exchanged vermiculite characterized by the ETA and compare their character and intensity. TG, DTA and XRD were used for the interpretation of ETA results and models.

Experimental

Starting material

The vermiculite (from the locality Santa Olalla, Huelva, Spain) with a half-unit cell composition $Mg_{0.439}(Si_{2.64}Al_{1.36})(Mg_{2.48}Fe^{3+}_{0.324}Fe^{2+}_{0.036}Al_{0.14}Ti_{0.01})O_{10}(OH)_2$ was used as a starting material [13]. Large flakes were ground using a Knife-mill (Netzsch ZSM-1, Germany) and sieved. Vermiculite particles with a size smaller than 80 μm were used for the experiments.

Preparation and properties of chemically treated vermiculite samples

The Na^+-saturated sample was prepared from the natural Mg^{2+}-vermiculite by a repeated contact with a 1 M NaCl solution under stirring at room temperature. Finally, the sample was washed with distilled water until the supernatant solution became free of Cl^-. The NH_4^+-saturated vermiculite was prepared from the Na^+-vermiculite by the repeated contact with a 1 M ammonium acetate solution (pH=7) at room temperature. The excess of ammonium acetate was subsequently washed out with distilled water and the slurry was separated by centrifugation. The presence of the NH_4^+-vermiculite was proved by XRD.

The natural Mg^{2+}-vermiculite has a surface area of 7 $m^2\ g^{-1}$. The ion exchange of Mg^{2+} for Na^+ and NH_4^+ ions caused an increase of the surface area to the values of 18.7 and 22.5 $m^2\ g^{-1}$, respectively. All vermiculite samples were dried in air at room temperature prior to the characterization.

Methods used for samples characterization

Emanation thermal analysis (ETA) [5–7] involves the measurements of radon release rate from samples previously labelled. The samples for ETA were labelled by soaking with acetone solution containing traces of ^{228}Th and ^{224}Ra nitrates. The specific activity of a sample after labelling was 10^5 Bq g^{-1}. Atoms of ^{220}Rn were formed by the spontaneous alpha decay of ^{228}Th and ^{224}Ra. The ^{224}Ra and ^{220}Rn atoms were incorporated into the sample to a maximum depth of 80 nm due to the recoil energy (85 keV/atom), which the atoms gain by the spontaneous α-decay. The maximum depth of ^{220}Rn penetration was 80 nm as calculated with the TRIM code [14].

The ETA measurements were performed on samples during heating in air at a heating rate of 6 K min^{-1}, using a modified Netzsch ETA-DTA instrument, Model 404. During the ETA measurements the labelled sample of 0.1 g was situated in a corundum crucible with a constant overflow of dry air (flow-rate 40 mL min^{-1}), which carried the radon

released from the sample into the measuring chamber of radon radioactivity. Details of the ETA measurements and data treatment has been described elsewhere [6, 7, 12].

TG/DTA measurements were carried out using Setaram Equipment (Model 2000) in the same experimental conditions as the ETA measurements.

High temperature X-ray powder diffraction patterns were measured on a Philips (X'Pert) diffractometer with a high temperature chamber (HTK 1200, Anton Paar) using Ni-filtered CuK_{α} radiation and a position sensitive detector (ASA-S, MBraun). Identical conditions for sample heating as for the thermal analysis measurements were used.

The surface area was determined by adsorption of nitrogen by the B.E.T method using the automatic system Micrometrics ASAP 2010.

Results and discussion

The initial information about thermal behavior of the vermiculite samples was obtained by XRD, TG and DTA. The results of these methods are compared in this paper with the ETA results, which characterized microstructure changes of the samples under in situ conditions of heating.

Natural Mg^{2+}-vermiculite

X-ray diffraction patterns (Fig. 1a and Table 1) show that at room temperature the natural Mg^{2+}-vermiculite is characterized by the interlayer distance of 14.4 Å. After heating to 125 and 225°C the interlayer distance decreased to 11.6 and 10.25 Å, respectively. It is assumed that these interlayer distances reflected the presence of two, one and about zero number of layers of water in the interlayer of the vermiculite. From the value of the interlayer distance 10 Å, which corresponds to the sample heated to 250–650°C, it followed that nearly unsolvated Mg^{2+} ions were present in the natural vermiculites after heating to these temperatures. This is in agreement with literature data [15–19].

As it followed from TG and DTA results (Fig. 2a curves 1 and 2) the dehydration of natural Mg^{2+}-vermiculite took place in two steps in the temperature range 30–300°C. We assumed that the first step (on heating up to 125°C) corresponded to the release of physically adsorbed water and a part of water molecules, which were not in the immediate contact with Mg^{2+} ions. In agreement with other authors [15–18] the second dehydration step observed on heating up to 200–250°C corresponded to the release of water molecules, which were in intermediate contact with Mg^{2+} ions.

ETA results (curve 3 in Fig. 2a) are in agreement with the above findings. The increase of the radon release rate (*E*) observed in the temperature ranges from 40 to 130°C and from 180 to 220°C is explained by the promoting effect of the water release on the release of radon, situated in the near surface layers and in the interlayer space of vermiculite. On the other hand, the decrease in the emanating rate *E* observed in curve 3, Fig. 2a was due to partial and total collapse of the interlayer gap, which took place after the first and second dehydration step of vermiculite, respectively.

Table 1 Interlayer spacing of vermiculite samples heated to various temperatures

	Temperature/°C	Interlayer spacing *d*/Å
Mg^{2+}-vermiculite	25	14.4
	125	11.6
	225	10.25
	325	10.15
	650	10
	750	9.98/9.2
	850	9.98
Na^{+}-vermiculite	25	12.16
	225	9.99
	325	9.99
	500	9.86
	900	9.69
	950	9.67
NH_4^{+}-vermiculite	25	10.7
	225	10.6
	325	10.54
	500	10.45
	700	10.27/9.2
	775	10.18/9.09
	825	9.11

In more detailed description we can state that the break observed on the ETA curve at 140°C and the following decrease of the radon release rate characterized the decrease of the interlayer gap of the partially dehydrated sample. The decrease of the radon release rate on sample heating above 240°C was ascribed to the collapse of the interlayer gap, accompanying the second dehydration step i.e. the release of water molecules, which were in intermediate contact with Mg^{2+} ions in the vermiculite. From the comparison of ETA and TG curves it followed that the collapse of the interlayer space of the vermiculite structure took place simultaneously with the release of remaining water molecules from the interlayer space. This interpretation is in agreement with XRD patterns (Fig. 1a) obtained under heating of the Mg vermiculite sample under similar conditions as used for TG, DTA and ETA measurements.

Moreover, from curve 3 in Fig. 2a it followed that no microstructure changes were revealed by ETA on heating of Mg^{2+}-vermiculite in the temperature range 300–590°C. The decrease of radon release rate, *E*, observed in the temperature range 590–900°C was ascribed to the formation of a well crystalline structure, after the departure of structural OH groups. The mass decrease due to the sample dehydroxylation was observed by TG above 650°C (Fig. 2a, curves 1 and 2).

The enhanced radon release on sample heating above 900°C indicated the formation of new phases, which is in agreement with the DTA and XRD results. The DTA effect observed in the temperature range from 700 to 850°C (Fig. 2a, curve 1), corresponded to the formation of enstatite (which was determined by XRD patterns in the sample heated to 850°C). It was reported earlier [11] that on further heating up to 1100°C the increase in the crystallinity of enstatite phase and also formation of the spinel phase took place.

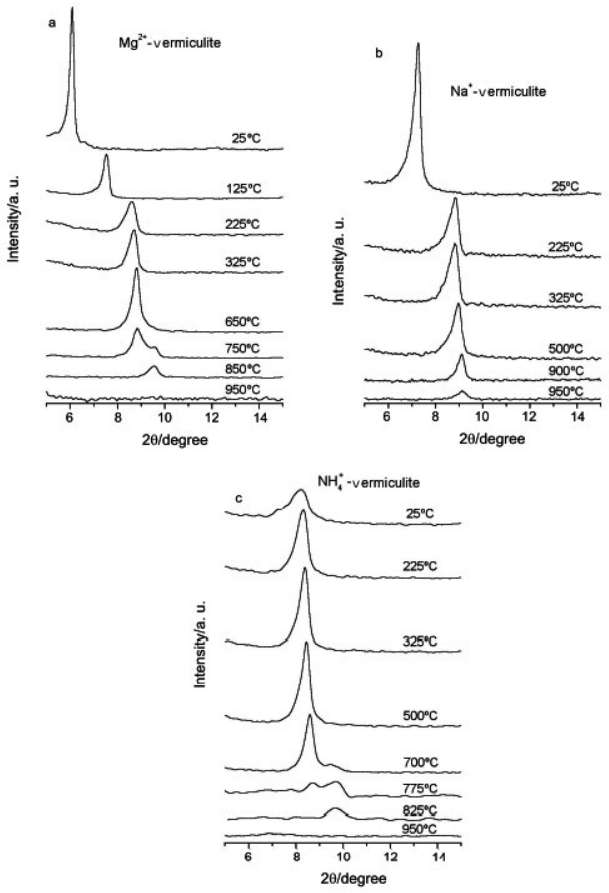

Fig. 1 XRD patterns of a – natural Mg^{2+}-vermiculite, b – Na^{+}-vermiculite and c – NH_4^{+}-vermiculite heated to different temperatures

We assumed that the formation of new phases (mainly enstatite) and interface boundaries led to the increase of the radon diffusion channels observed during sample heating above 900°C and that, in its turn, the increase of crystallites of the newly formed phase led to the decrease of the number of radon diffusion channels, which was characterized by a decrease of the radon release rate.

Na^{+}-saturated vermiculite

The Na^{+}-vermiculite sample used in this study has a single water layer (layer distance about 12 Å, Table 1). In agreement with the literature data [18] we determined by XRD that after dehydration the interlayer distance decreased to 9.99 Å. From the ETA results (curve 3 in Fig. 2b) it followed that the increase in the radon release rate, *E*, during the dehydration of the sample was followed by a sharp decrease of *E*, which

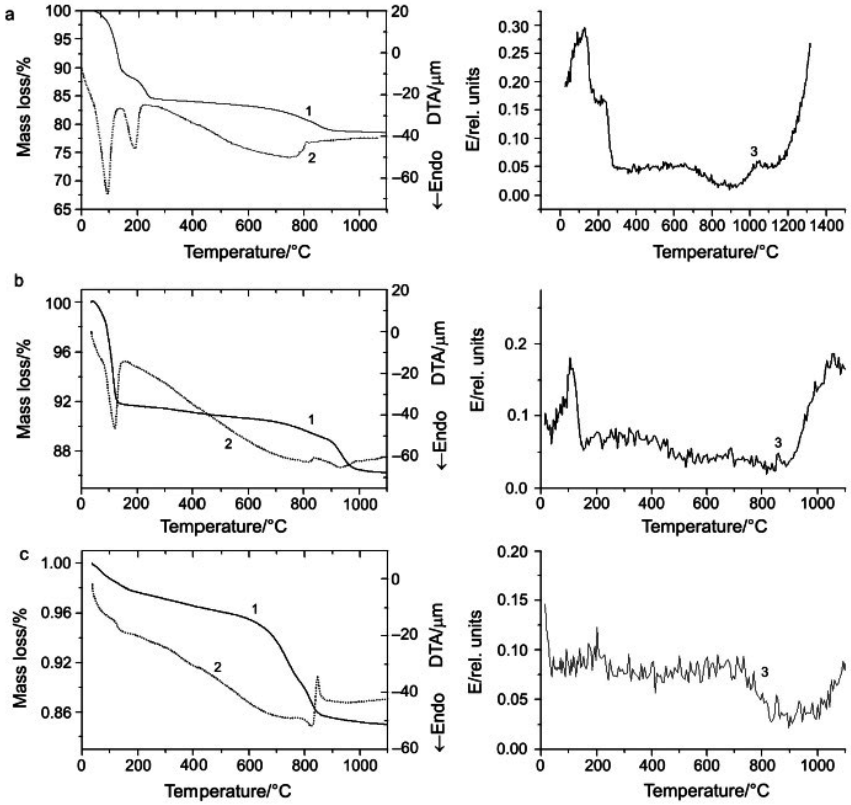

Fig. 2 Results of thermogravimetry, (curve 1), DTA (curve 2) and ETA (curve 3) of natural and chemically treated vermiculite samples obtained on heating in air at the rate 6 K min^{-1}. a – natural Mg^{2+}-vermiculite, b – Na^{+}-vermiculite c – NH_4^{+}-vermiculite

indicated the decrease in the interlayer gap. The onset temperature of the collapse of the interlayer gap was determined at 110°C. The decrease of *E*, observed above 400°C, indicated the thermal annealing/ordering of the structure after the release of structural OH groups. The XRD pattern (Fig. 1b and Table 1) characterized the interlayer distance of Na^{+}-vermiculite heated to 500°C as 9.86 Å.

The mass loss and heat effects observed by TG and DTA, respectively in the temperature range 850–975°C, (curves 1 and 2 in Fig. 2b) corresponded to the formation of the new phase enstatite. Moreover, a new phase (determined by XRD as fosterite) was observed in the Na^{+}-vermiculite heated to 1100°C [11].

NH_4^+-*saturated vermiculite*

From XRD (Fig. 1c and Table 1) it followed that the NH_4^+-saturated vermiculite has the interlayer distance of 10.7 Å, indicating that there is nearly no water in the interlayer space and that the ammonium ions may be strongly bound to the silicate layers. For the sample heated to 225 and to 325°C the interlayer spacings determined by XRD were 10.6 and 10.54 Å, respectively (Table 1). This is in support of our TG and DTA results (curves 1 and 2 in Fig. 2c) where only a small water loss was observed in this temperature range. We assumed that the slow mass loss observed in the temperature range from 40 up to 200°C corresponded to the liberation of water from voids, which was accompanied by a small increase in radon release rate *E*.

The mass loss observed in the range of 600–830°C was ascribed to the release of ammonia and OH groups. The decrease of the radon release rate observed in the range 730–830°C (curve 3 in Fig. 2c) was ascribed to the annealing of structure irregularities of the vermiculite sample after the release of ammonia and remaining OH groups. This is agreement with the finding presented in [20].

Modelling and evaluation of the ETA results

In the modelling of the migration of radon atoms, which were used as a microstructure probe of solids, we supposed that structure irregularities served as channels for radon migration.

Following expression was proposed [12] for the modelling of radon migration in course of solid-state processes in solids:

$$E(T)=E_0+\sum_{i=1}^{n} p_i D_{i0} \exp\left(-\frac{Q_i}{2RT}\right)+\sum_{j=1}^{m} p_j D_{j0} \exp\left(-\frac{Q_j}{2RT}\right)\Psi_j(T) \qquad (1)$$

The functions $D(T)$ and $\Psi(T)$ are determined by the mechanisms of chemical or physical process.

If number of radon diffusion paths and/or surface area decreases, the structural function $\Psi(T)$ has a descending character, whereas if the number of radon diffusion paths increases during the sample heating, the structural function $\Psi(T)$ has an increasing character. According to Beckman and Balek [12], the decreasing $\Psi(T)$ function in Eq. (2) was used for the description of changes in the amount of the structure defects in solids.

$$\Psi(T)=0.5\left[1+erf\left(\frac{1-T_m/T}{(\Delta T\sqrt{2})/T}\right)\right] \qquad (2)$$

where *erf* is the sign for the integral Gauss function (error function), T_m is the temperature of maximal rate of the annealing of the defects which serve as radon diffusion paths, ΔT_m is the temperature interval of the respective solid state process.

Figures 3a–3c demonstrated the comparison of the ETA experimental results (as dots –curve 1) with the results of mathematical modeling (curve 2) of the changes of the radon release rate during heating of natural Mg^{2+}-vermiculite, the Na^+-saturated vermicu-

lite and the NH_4^+-saturated vermiculite samples. It is obvious from Figs 3a–3c that a good agreement was reached between the experimental and model curves. In the modelling we supposed that the interlayer gap as well as grain boundaries of the vermiculite served as radon diffusion channels.

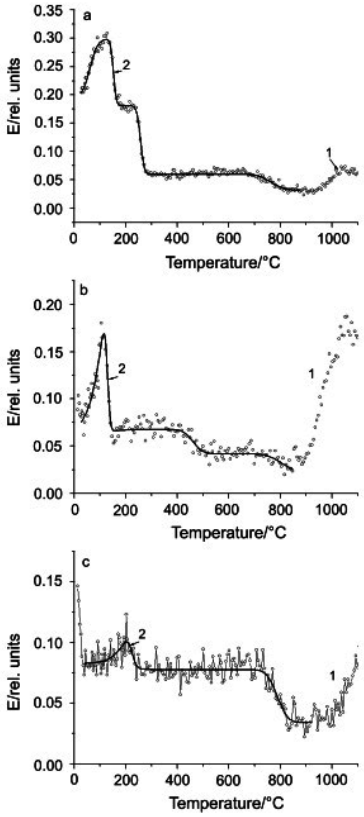

Fig. 3 Comparison of ETA experimental results (curve 1 – dots) with temperature dependences of radon release rate in the selected temperature intervals obtained by modelling (curve 2). a – natural Mg^{2+}-vermiculite, b – Na^+-vermiculite c – NH_4^+- vermiculite

In Figs 4a–4c we separately present the $\Psi(T)$ functions characterizing the thermal behavior of all three vermiculite samples studied. Curves 1, 2 and 3 represent the $\Psi_i(T)$ functions in the respective temperature intervals characterizing the decease in the interlayer space after the release of water molecules and/or to the ordering of the structure after the departure of structural OH groups and ammonia. Curves 1', 2' and 3' correspond to the respective $d\Psi_i/dT$. The temperature ranges of the segments indicated by ETA curves, where microstructure changes in the studied vermiculite samples took place are listed in Table 2.

Table 2 Characterization of effect of ion exchange on microstructure changes of vermiculite samples as obtained by evaluation of ETA results

	Mg^{2+}-vermiculite			Na^{+}-vermiculite			NH_4^{+}-vermiculite	
Temperature range of the ETA segment	25–190	190–330	380–900	30–200	200–580	580–950	40–300	300–950
Onset and final temperature of microstructure changes determined from $\Psi_i(T)$ function	120–190	210–315	630–900	90–160	340–550	600–900	180–270	680–890
T_{max}/°C	151	256	764	126	460	802	219	788
$\Psi_i(T_{max})/\Psi(T)$/%	12.0	12.1	2.9	10.0	3.6	1.9	4.5	4.4
Q_D/kJ mol^{-1}	74.7	–	–	53.5	–	–	43.8	–
ΔH/kJ mol^{-1}	33.1	41.5	82.7	31.3	58.0	85.8	38.5	84.7

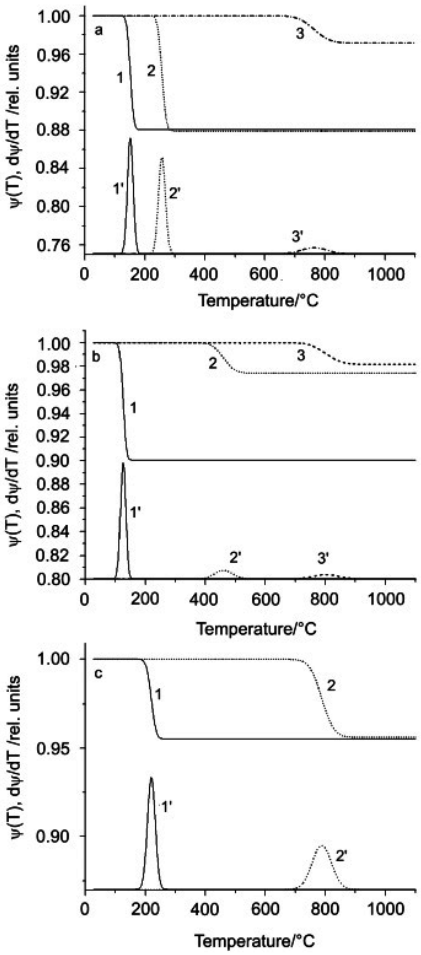

Fig. 4 Temperature dependences of $\Psi_i(T)$ functions characterizing the annealing of radon diffusion channels due to microstructure changes in a – natural Mg^{2+}-vermiculite, b – Na^+-vermiculite, c – NH_4^+- vermiculite. Curves 1, 2 and 3 represent the $\Psi_i(T)$ functions in the selected temperature intervals characterizing the decrease in the interlayer space after the release of water molecules and/or to the ordering of the structure after the departure of structural OH groups and ammonia, respectively. Curves 1', 2' 3' correspond to the respective $d\Psi_i/dT$

The temperature dependences of $\Psi_i(T)$ functions, characterized the annealing of the interlayer gaps in partially or totally dehydrated vermiculite and/or the formation of a well crystalline structure after the departure of structural OH groups. Table 2 contains also the information about onset and final temperatures of microstructure changes, as determined from each $\Psi_i(T)$ function.

The temperatures T_{max}, which indicate the maximal rate of the interlayer gap collapse and the annealing of respective radon diffusion paths are also presented in Table 2 together with the parameter $(\Psi_i T_{max})/\Psi T$, characterizing the relative intensity of the annealing process in the respective temperature ranges.

The computer treatment of ETA experimental data made it possible to characterize the diffusion of radon in the first ETA segments where the radon diffusion was enhanced by the release of water from the vermiculite samples. Moreover the values ΔH of enthalpy of the microstructure changes due to decrease or collapse of interlayer gaps were determined from the mathematical model for the corresponding temperature intervals. The values of activation energy of radon diffusion Q_D determined by modelling are presented for all three vermiculite samples in Table 2. The detailed discussions of the values will made in next paper. In this study we should just point out that after evaluation of the ETA results (Table 2) we can assess the effect of the ion exchange on the microstructure development of the vermiculite samples.

The values of the interlayer space of vermiculite samples determined by XRD were in an agreement with the ETA characteristics. Moreover from the comparison of the results it followed that the ETA is more sensitive than XRD to the microstructure changes and to the annealing of near surface structure irregularities of vermiculite samples.

Conclusions

It was demonstrated that the changes in the radon release rate observed by ETA, which reflected the decrease and collapse of the interlayer space after the release of water as well as the formation of new crystalline phases were in a good agreement with the results of TG and DTA and XRD. The model used for the evaluation of the ETA experimental results was found suitable for the quantitative characterization of microstructure changes during in situ conditions of heating of clay minerals. From the results of the modelling we can recommend the $\Psi(T)$ functions as a suitable tool for the characterization of the decrease of radon diffusion paths due to decrease of interlayer gap in vermiculite samples and the annealing of the structure disorder after the release of hydroxyls and ammonia, respectively.

* * *

This publication was prepared on the basis of the results obtained in the frame of the Project No. LN00A028 supported by the Ministry of Education of the Czech Republic and the Project n° 1999-095 supported by the CICYT of Spain. Two of the authors (I.M.B and I.N.B.) express their thanks to the NATO Science Fellowship Programme for the support of their stay at Řež (CZ).

References

1 J. R. Hindman, Vermiculite, in: Industrial Minerals and Rocks, (D. D. Carr, Ed.) Society for Mining, Metallurgy and Exploration, Inc., Littleton, Colo., USA 1994, p. 1103.
2 J. Konta, Appl. Clay Sci., 10 (1995) 275.

3 A. Russell, Vermiculite in Industrial Minerals, Annual Supplement, Mining Journal, London, Vol. 332, 1998, p. 8.
4 M. J. Potter, Amer. Ceram. Bull., 1999, 145.
5 V. Balek. and J. Tölgyessy, Emanation Thermal Analysis and other radiometric emanation methods. In:Wilson and Wilson's Comprehensive Analytical Chemistry, Vol. XIIC, (G. Svehla, Ed.), Elsevier, Amsterdam 1984, pp. 304.
6 V. Balek, Thermochim. Acta, 192 (1991) 1.
7 V. Balek, J. Šubrt, T. Mitsuhashi, I. N. Beckman and K. Györyová, J. Therm. Anal. Cal., 67 (2002) 15.
8 Z. Málek, V. Balek, D. Garfinkel Shweky and S. Yariv, J. Thermal Anal., 48 (1997) 83.
9 V. Balek, Z. Málek, S. Yariv and S. Matuschek, J. Therm. Anal. Cal., 56 (1999) 67.
10 V. Balek, Z. Málek and E. Klosová, J. Therm. Anal. Cal., 53 (1998) 625.
11 J. Poyato, L. A. Perez-Maqueda, M. C. Jimenez de Haro, J. L. Pérez-Rodríquez, J. Šubrt and V. Balek, J. Therm. Anal. Cal., 67 (2002) 73.
12 I. N. Beckman and V. Balek, J. Therm. Anal. Cal., 67 (2002) 49.
13 L. A. Pérez-Maqueda, O. B. Caneo, J. Poyato and J. L. Pérez-Rodríquez, Phys. Chem. Minerals, 28 (2001) 61.
14 J. F. Ziegler, J. P. Biersack and U. Littmark, The Stopping and Range of Ions in Solids, Pergamon Press, New York 1985.
15 G. F. Walker, Clays and Clay Minerals, 4 (1956) 101.
16 G. F. Walker and W. F. Cole, The vermiculite minerals, In The Differential Thermal Investigation of Clays, Chapter 7, (R. C. Mackenzie, Ed.), Mineralogical Society, London 1957, pp. 191–206.
17 J. Keay and A.Wild, Clay Minerals Bulletin, 4 (1961) 221.
18 H. van Olphen, Clays and Clay Minerals, 11 (1963) 178.
19 H. van Reichenbach, Clay Minerals, 29 (1994) 327.
20 J. Poyato, L. A. Pérez-Maqueda, A. Justo and V. Balek, Clays Clay Miner., 50 (2002) 791.